Melanosome Morphologies in Murine Models of Hermansky–Pudlak Syndrome Reflect Blocks in Organelle Development

Thuyen Nguyen, Edward K. Novak,† Maryam Kermani, Joachim Fluhr, Luanne L. Peters,* Richard T. Swank,† and Maria L. Wei

Department of Dermatology, Veterans Affairs Medical Center, University of California, San Francisco, CA, U.S.A.; *Jackson Laboratory, Bar Harbor, ME and †Department of Molecular and Cellular Biology, Roswell Park Cancer Center, Buffalo, NY, U.S.A.

Hermansky–Pudlak syndrome is an autosomal recessive disease characterized by pigment dilution and prolonged bleeding time. At least 15 mutant mouse strains have been classified as models of Hermansky–Pudlak syndrome. Some of the genes are implicated in intracellular vesicle trafficking: budding, targeting, and secretion. Many of the Hermansky–Pudlak syndrome genes remain uncharacterized and their functions are unknown. Clues to the functions of these genes can be found by analyzing the physiologic and cellular phenotypes. Here we have examined the morphology of the melanosomes in the skin of 10 of the mutant mouse Hermansky–Pudlak syndrome strains by transmission electron microscopy. We demonstrate that the morphologies reflect inhibition of organelle maturation or transfer. The Hermansky–Pudlak syndrome strains are classified into morphologic groups characterized by the step at which melanosome biogenesis or transfer to keratinocytes is inhibited, with the cappuccino strain observed to be blocked at the earliest step and gunmetal blocked at the latest step. We show that all Hermansky–Pudlak syndrome mutant strains except gunmetal have an increase in unpigmented or hypopigmented immature melanosomal forms, leading to the hypopigmented coat colors seen in these strains. In contrast, the hypopigmentation seen in the gunmetal strain is due to the retention of melanosomes in melanocytes, and inefficient transfer into keratinocytes. ***Key words: melanocytes/organelle biogenesis/pigmentation J Invest Dermatol 119: 1156–1164, 2002***

The Hermansky–Pudlak syndrome (HPS) is observed in humans and mice and is caused by mutations in genes that regulate the biogenesis of lysosomes and lysosome-related organelles such as melanosomes and platelet-dense granules (Dell'Angelica *et al*, 2000), which suggests that these seemingly disparate organelles share a common pathway of biogenesis or maturation. The resulting defects in these organelles cause prolonged bleeding and oculocutaneous albinism in affected individuals (Huizing *et al*, 2000). HPS exhibits genetic heterogeneity: in humans, four genes have been cloned, and each when defective in isolation gives rise to a clinical syndrome classified as HPS. In mice, at least 15 HPS genes have been noted (Swank *et al*, 1998).

Whereas the functions of many of the HPS gene products remain unknown, it is likely that most of them will function in vesicle/organelle biogenesis and membrane trafficking along the pathway of melanosome formation. The functions of five genes (*Ap3b1*, *Ap3d*, *Pldn*, *Rabgtta*, *Rab27a*) have been implicated in vesicle/organelle formation and trafficking. *Ap3b1* and *Ap3d* encode subunits of the adaptor complex AP3 (Kantheti *et al*, 1998; Dell'Angelica *et al*, 1999; Feng *et al*, 1999), which binds to endosomes and the *trans*-Golgi network. A neuronal-specific isoform of AP3 is required for synaptic vesicle formation from endosomes (Faundez *et al*, 1998). *Pldn* (palladin) protein binds syntaxin 13 (Huang *et al*, 1999), a member of the family of soluble *N*-ethylmaleimide-sensitive factor attachment protein receptors (SNARES), which mediate fusion of intracellular membranes. *Rabgtta* encodes a subunit of a Rab geranylgeranyl transferase (Detter *et al*, 2000), and is required for efficient polarization of cytolytic T cell granules (which are also specialized lysosome-like organelles) to the immunologic synapse (Stinchcombe *et al*, 2001). *Rab27a* encodes a member of the family of GTPases that controls intracellular vesicular transport (Novick and Zerial, 1997; Chavrier and Goud, 1999) and is required for melanosome transport from the cell body to the dendritic processes (Wilson *et al*, 2000; Bahadoran *et al*, 2001; Hume *et al*, 2001). In mice with defective *HPS1, HPS3, HPS4*, *Pldn*, or *mu* genes, melanosomes in eye tissue have been observed to be abnormal (Ito *et al*, 1982; Gardner *et al*, 1997; Suzuki *et al*, 2001, 2002; Zhang *et al*, 2002a).

Eukaryotic cells are distinguished by the presence of membrane-bound organelles. The study of organelle biogenesis has been greatly advanced by the study of organisms such as *Saccharomyces cerevisiae* and *Drosophila melanogaster* that exhibit mutations in genes that regulate organelle development (Dell'Angelica *et al*, 2000). Morphologic studies of yeast cells bearing mutations in genes that govern the biogenesis of the yeast vacuole (an organelle analogous to the mammalian lysosome) have helped to

Manuscript received August 18, 2002; revised September 6, 2002; accepted for publication September 12, 2002

Reprint requests to: Dr Maria L. Wei, Dermatology Service (190), Veterans Affairs Medical Center, 4150 Clement Street, San Francisco, CA 94121, U.S.A. Email: mlwei@orca.ucsf.edu

Abbreviations: HPS, Hermansky–Pudlak syndrome; TEM, transmission electron microscopy; Tyrp1/TRP-1, tyrosinase-related protein 1; TRP-2, tyrosinase-related protein 2.

identify and classify more than 40 genes that were involved (Banta *et al*, 1988; Raymond *et al*, 1992; Wada *et al*, 1992). Although the human *HPS1*, *HPS3*, and *HPS4* genes have no sequence homologs in yeast, the *HPS2/Ap3b1* gene has a yeast homolog and some of the as yet uncharacterized mouse genes may have yeast homologs as well. HPS mutations result in mammalian diseases due to defects in organelle biogenesis. We have undertaken the current morphologic study in order to characterize and classify HPS mouse strains as a step towards understanding HPS gene product function.

The melanosome is an organelle uniquely suited for morphologic examination in tissue samples by transmission electron microscopy (TEM) due to its electron-dense pigmentation. Other organelles consistently affected in HPS are not readily amenable to examination by TEM. Platelet-dense granules in HPS lose their electron density (Witkop *et al*, 1987) and lysosomes are only easily identified after internalization of electron-dense material or by antibody labeling, and thus are more difficult to identify in tissue samples.

The melanosome has four distinct stages of maturation (Nordlund *et al*, 1998), stages I–IV. Type I melanosomes have intralumenal vesicles (Raposo *et al*, 2001) and resemble multivesicular bodies, structures found along the endosomal pathway. Type II is characterized by an elongated, elliptical shape, with intralumenal fine fibrils giving a striated appearance; type III exhibits pigment deposition along the fibrils, and type IV has dense pigmentation filling the organelle and obscuring the fibrillar structure (Seiji *et al*, 1963). In normal melanosome development, the type I melanosome is distinguished by its accumulation of the Pmel17/gp100 protein (*silver* locus product) (Kushimoto *et al*, 2001; Raposo *et al*, 2001; Raposo and Marks, 2002), which is cleaved and localized to the intralumenal vesicles (Berson *et al*, 2001). Two enzymes involved in pigment synthesis, Tyrp1/ tyrosinase-related protein (TRP)-1 and dopachrome tautomerase/TRP-2, may also be in the type I melanosome, but appear to be inactivated in this compartment by proteolytic cleavage (Kushimoto *et al*, 2001). Pmel17/gp100 functions in the formation of the melanosomal striations and elongated shape to give rise to the type II melanosome (Berson *et al*, 2001). Subsequently, pigment synthesis and deposition along the striations lead to the appearance of type III and IV forms. Whereas HPS-affected individuals exhibit pigment dilution, pigment is not absent, as a functional tyrosinase enzyme, necessary and sufficient for pigment formation, is present.

We examined melanosomes in the skin of HPS mice, classified the mice by the stage of organelle maturity and demonstrated that the defective genes result in blocks in melanosome development or transfer to keratinocytes.

MATERIALS AND METHODS

Mice Dorsal back skin samples from 4 wk old mice were harvested. The mutant mice and their corresponding control strain, C57BL/6, C3H/HeJ, or C57BL/10J were analyzed. All of the mutants arose spontaneously, most on the C57BL/6 background; others were bred into the C57BL/6 genotype (Novak *et al*, 1980, 1984; Gibb *et al*, 1981; Zhang *et al*, 2002b). The cappuccino strain arose on the C3H/HeJ background (Gwynn *et al*, 2000). The cocoa mouse arose on the C57BL/10J background (Novak *et al*, 1988). The three control strains had very similar melanosome morphology (data not shown), so C57BL/6 was used as a representative control. The HPS mice examined and the corresponding human diseases and genes are listed in **Table I**. All animal procedures were approved by Institutional Animal Care Use Committee.

Measurement of coat color The dorsal back coat pigmentation (P) was measured using a Mexameter MX 18 (Courage & Khazaka, Cologne, Germany), which gives a calculated value of melanin content based on the absorption of light emitted at 568 nm and 880 nm. Background was subtracted by subtracting P_{tyr}, the coat color measurement for the white albino mouse C57BL/6J-*Tyr*$^{c-2J}$ (TyrG291 T), which is lacking tyrosinase activity and has no pigment production. A comparison with the coat pigment of the control strain (P_{con}) was done:

$$\text{Percent pigment} = (P - P_{tyr})/(P_{con} - P_{tyr}) \times 100$$

Electron microscopy Tissue was fixed in modified Karnovsky's fixative (2% paraformaldehyde/2% glutaraldehyde/0.1 M cacodylate buffer, pH 7.3/ 0.06% $CaCl_2$) for 24 h, washed twice in 0.1 M cacodylate buffer, postfixed in reduced osmium (1.5% potassium ferrocyanide/2% osmium tetroxide) for 2 h, rinsed in H_2O, dehydrated with increasing ethanol concentrations, and embedded in Epon resin. Grids were stained in 10% uranyl acetate/ 50% methanol. Cross-sections of melanosomes were measured at $\times$ 50,000 magnification for major axis and minor axis, in order to assess relative size and shape. Images of a calibration grid were taken to control for any variability in magnification. Melanocytes were identified by their organization in hair follicles, as well as their lack of keratin filaments and desmosomes (both are present in keratinocytes). Each melanosome was measured and classified by morphology, i.e.: (i) multiple intralumenal vesicles present, no pigment or striations seen; (ii) striated matrix present, round cross-section; (iii) striated matrix, elliptical cross-section; (iv) fully pigmented, round cross-section; and (v) fully pigmented, elliptical cross-section. Noted also were any melanosomal features unique to any particular strain. For each strain at least 100 melanosomes were examined in each of at least two different animals. Statistical analysis of five control mice revealed no interanimal variance.

Statistical analysis Statistics were calculated with Prism3 (GraphPad, San Diego, CA). The data were tested for normal distribution and in the case of more than two groups an ANOVA with *post-hoc* pairwise comparison was calculated (Bonferroni or Dunn's test, respectively).

RESULTS

HPS mouse strains have varying coat colors In HPS patients, it has been observed that the pigment dilution can have wide variation, and at times can be quite subtle (Huizing *et al*, 2000). The assessment of gene effects in patients can be complicated by variations in genetic backgrounds. This factor can be eliminated by studying inbred mice, when mutant strains share a common genetic background, as is the case for most of the HPS murine strains. The HPS mouse strains were also observed to have a range of pigment dilution. The strains can be

Table I. Mouse models of the Hermansky-Pudlak Syndrome

Mouse Strain	Human disease	Gene product	Function
pale ear	HPS1	HPS1	?
pearl	HPS2	AP3 ß3A submit	Protein sorting to lysosomes and lysosome-like organelles
cocoa	HPS3	HPS3	?
light ear	HPS4	HPS4	?
pallid	?	pallidin	Binds to syntaxin 13 SNARE
gunmetal	?	Rab geranylgeranyl transferase α subunit	Rab prenylation
ruby eye	?	?	?
ruby eye-2	?	?	?
reduced pigmentation	?	?	?
cappuccino	?	?	?

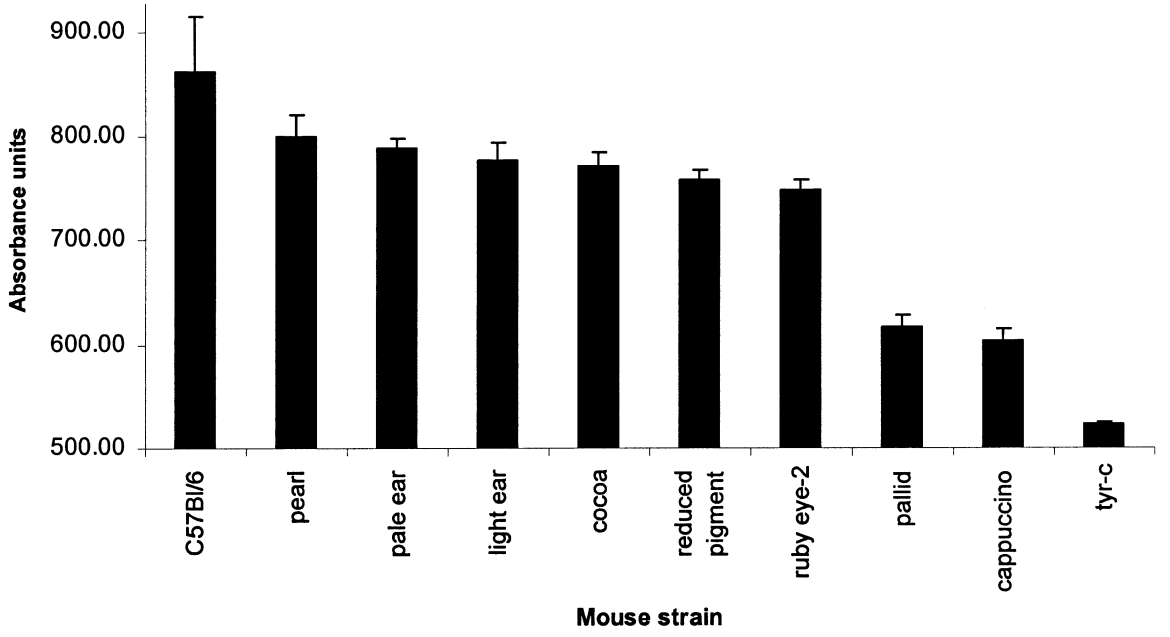

Figure 1. Coat color variation in HPS strains. Pigmentation was measured using a Mexameter. Tyr-c, tyrosinase activity-negative mouse strain C57BL/6J-*Tyr*$^{c-2J}$ (TyrG291T) whose melanosomes are devoid of pigment. Error bars represent SD.

separated into two groups by coat color. The first group varies from dark to light shades of gray. This group consists of gunmetal, pearl, pale ear, light ear, cocoa, reduced pigmentation, ruby eye, and ruby eye-2. As noted previously (Swank *et al*, 1998), the pale ear and light ear strains were identical in coat color and in having hypopigmented ears and tails. It is somewhat difficult to discern cocoa from reduced pigmentation, and ruby eye and ruby eye-2 are indistinguishable from one another by coat and eye color. The second group, consisting of pallid and cappuccino, is very hypopigmented, with hues in the off-white or cream-colored category.

It is possible that the coat color in these strains is an effective marker for the severity of the defect in the biogenesis of the melanosome, and of similarly affected organelles such as the platelet-dense granule and the lysosome. In order to quantitate the pigment dilution in these HPS strains, the coat color was measured (**Fig 1**). The relative ranking of the strains by Mexameter readings correlates well with the color ranking discerned by eye.

Murine HPS strains can be grouped by melanosomal morphology Melanosomes in follicular melanocytes were identified and examined by TEM (**Fig 2**). In the parental C57BL/6 strain (**Fig 2*C***), a mixture of both ellipsoidal and spherical type IV fully pigmented melanosomes predominate. Striated type II and III forms are also readily seen. Very few to no spherical multivesicular bodies are seen.

A strikingly immature melanosomal phenotype was observed in the cappuccino and pallid strains (**Fig 2**; *cno, pa*), the two strains that had the most hypopigmented coat colors. In cappuccino the melanosomes were noticeably smaller than those seen in the parental strain, and were markedly abnormal. Very few type IV melanosomes were observed, either elliptical or spherical. Pigmentation appeared granular and irregularly deposited, compared with the fine pigment deposited evenly along the striations seen in the parental strain. All structures containing pigment were spherical, and often, the pigment was a small core within a larger limiting membrane. Few striated structures were observed, and multivesicular bodies were evident and abundant. In pallid, an increase in multivesicular forms was also observed, and whereas relatively more striated forms were seen in comparison with cappuccino, these forms were generally misshapen and had irregular pigmentation.

A second group of mouse strains (cocoa, ruby, ruby eye-2, reduced pigmentation) appeared to have an intermediate maturation phenotype. These strains showed little to no evidence of ellipsoidal type IV melanosomes (**Fig 2**; *coa, ru, ru-2, rp*). Almost all fully pigmented forms were spherical. In addition, in some of these strains, an increase in the relative number of striated forms was evident, although these were not normally shaped type II and III melanosomes. In reduced pigmentation, the striated forms were elongated, but most were irregularly shaped and only approximated ellipsoidal shapes. In cocoa, ruby eye-2, and pallid, the striated forms were predominantly round in cross-section, suggesting that they remained spherical. Also, spherical multivesicular bodies were observed, in contrast to the relative paucity of such forms in the parental strain.

The pale ear, light ear, pearl, and gunmetal strains exhibited near normal phenotype by TEM. The melanosomes appeared quite similar to those in the parental strain, in that type IV fully pigmented melanosomes were the predominant form (**Fig 2**; *ep, le, pe, gm*). Type II and III forms were seen to a lesser extent than type IV melanosomes. Pearl, however, was distinguished from gunmetal, pale ear, light ear, and C57BL/6 by an apparent increase in melanosomal membrane blebbing, suggesting abnormal vesicular trafficking involving these melanosomes.

Melanosome biogenesis in the cappuccino and pallid strains is blocked at an early stage In each of the mouse strains, the major axis of type IV melanosomes were measured as an indication of mature melanosome size (**Fig 3*a***). The few, poorly formed type IV melanosomes from the cappuccino mouse were found to be significantly smaller than those measured in the parental strain. Most of the other strains exhibited mature melanosomes that were slightly smaller than the parental melanosome size.

The major axis of each of the immature melanosomal forms was also measured to quantitate the sizes of these forms (**Fig 3*b***), and to determine if there was an increase in size when melanosomes underwent maturation. In the parental cells, there is a clear progression in size from type II/III melanosomes to type IV. A less marked progression in size from precursor to

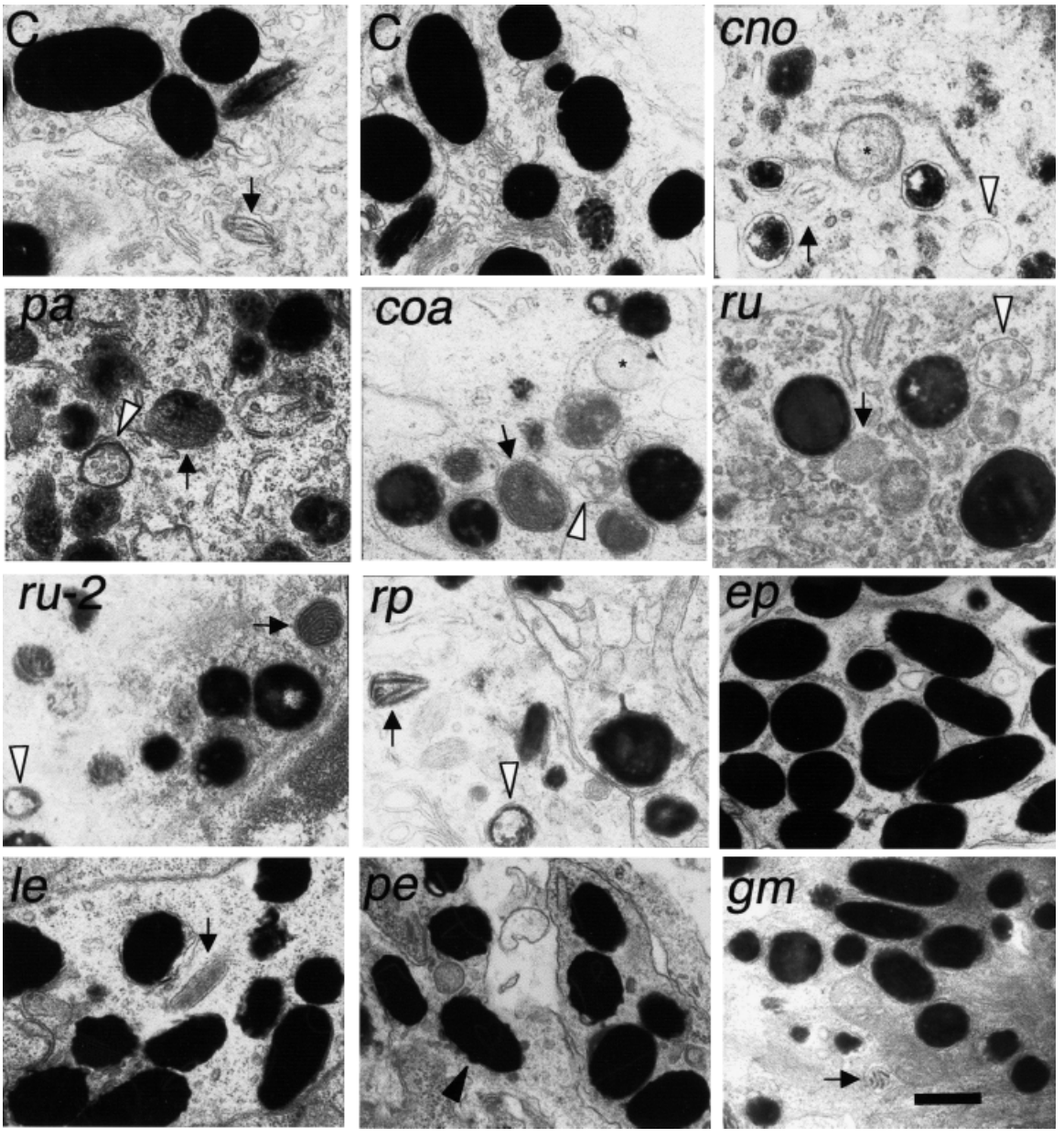

Figure 2. HPS mouse strains exhibit different degrees of aberrant melanosomal morphology. C, C57BL/6; *cno*, cappuccino; *pa*, pallid; *coa*, cocoa; *ru*, ruby eye; *ru-2*, ruby eye-2; *rp*, reduced pigmentation; *ep*, pale ear; *le*, light ear; *pe*, pearl; *gm*, gunmetal. The cappuccino strain is unique in having very small, abnormally pigmented structures. The fields were chosen to show representative forms of all melanosomal types for each strain, so do not necessarily demonstrate predominance of any specific melanosomal type. Asterisks, mitochondria. *White arrowheads*, multivesicular bodies; *arrows*, striated forms; *black arrowhead*, blebbing of the limiting membrane in pearl melanosomes. *Scale bar* = 0.5 μm.

mature melanosome was seen in most of the other strains. The increase in size was completely abolished in both the cappuccino and pallid strains, suggesting that melanosomal development was arrested at an early stage in these strains. Two additional strains, gunmetal and cocoa, also did not undergo a significant increase in size from type II/III to type IV forms.

The percentage of immature melanosomal forms is increased in HPS mouse strains As it appeared that the pallid and cappuccino strains were blocked at an early stage of melanosome development, it seemed likely that the remaining strains could also be blocked or inhibited at a morphologically distinct step in biogenesis, so a quantitative assessment of melanosomal maturity was done. One indication of degree of maturity could be shape, with immature spherical forms progressing to more mature elliptical forms. Therefore, the shape distribution of the type IV melanosomes was assessed (**Fig 4*a***). In C57BL/6 cells, there was a slight predominance of spherical vs elliptical forms (52% *vs* 48%). A similar distribution was seen in the light ear and pearl strains. Several strains (cocoa, reduced pigmentation, ruby eye, ruby eye-2, pallid, cappuccino) had a marked shift of distribution towards a predominance of spherical forms, suggesting that these strains had an increase in the percentage of immature forms. Two strains (pale ear and gunmetal) that we had identified as "near normal" on the basis of pigment content and overall morphology, had a shift in distribution towards more elliptical forms. The secretion of these elliptical type IV forms might be a rate-limiting step in these strains, or a rate-limiting step at an earlier point of biogenesis might cause an increase in elliptical type II/III forms.

To distinguish between these two possibilities, the relative numbers of the different melanosomal forms were quantitated.

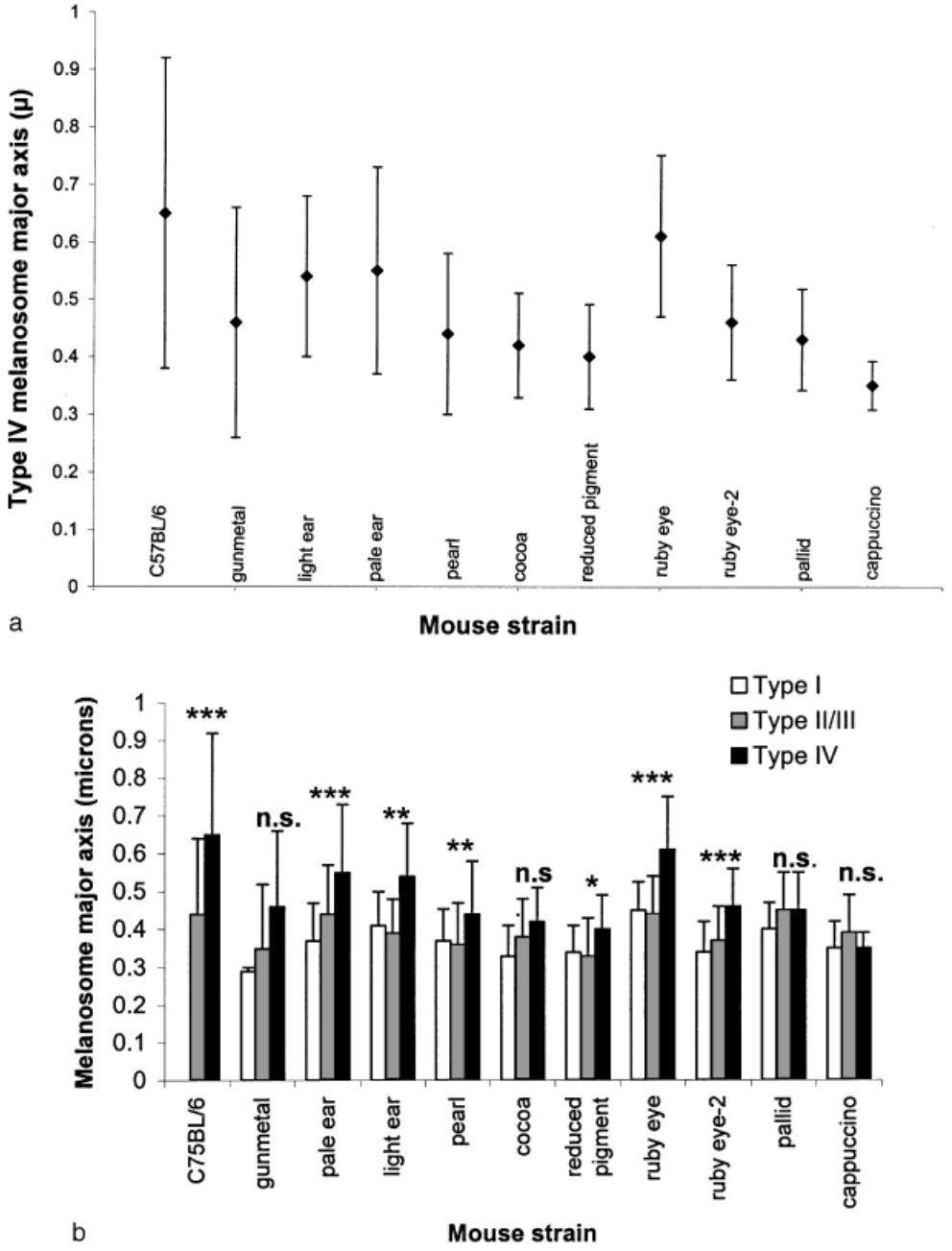

Figure 3. Comparison of HPS melanosome size. (*a*) Measurement of type IV melanosome major axes. Note the small size of melanosomes in cappuccino. (*b*) Measurements of major axes of all observed melanosomal types. (Data for type IV forms is taken from *a*.) Melanosomes in cappuccino and pallid do not undergo a size maturation. An ANOVA with *post hoc* pairwise comparisons (type I *vs* IV and II/III *vs* IV) were calculated for all strains (except C57BL/6, for which a pairwise t test was done as no type I melanosomes were noted). In the case of a significant ANOVA the following p-values were calculated in the *post-hoc* test: $^{*}p < 0.01$; $^{**}p < 0.001$; $^{***}p < 0.0001$; n.s., not significant. Error bars represent SD.

C57BL/6 was found to have the majority of melanosomes in the type IV form, with a minority in the type II/III form (**Fig 4*b***). In the HPS strains, an increased proportion of multivesicular structures was strikingly apparent, with a concomitant decrease in type IV forms. This finding was most marked in the cappuccino strain. The percentage of unpigmented multivesicular forms present in each strain was inversely proportional to the degree of pigmentation (**Fig 5**). Whereas there was a marked increase in immature forms in the pale ear strain, the increase in multivesicular forms seen in gunmetal was negligible, suggesting that the pigment dilution in this strain may be due to another cause, such as an inefficient transport and/or secretion of melanosomes.

Melanosomes accumulate intracellularly in the gunmetal strain In order to assess whether gunmetal had a defect in melanosome transport or secretion, the melanocytes were examined at a lower magnification in the gunmetal and control strains, and an increase in the number of intracellular melanosomes in the gunmetal melanocytes was noted (**Fig 6**). The number of melanosomes per unit area was quantitated and the density in gunmetal melanocytes was found to exhibit a 2.4-fold increase over the density of melanosomes observed in control melanocytes. Thus a significant accumulation of melanosomes was observed in gunmetal cells compared with that in control cells, and together with the data in **Fig 4(*a*,*b*)**, suggests that this is most likely due to a decrease in

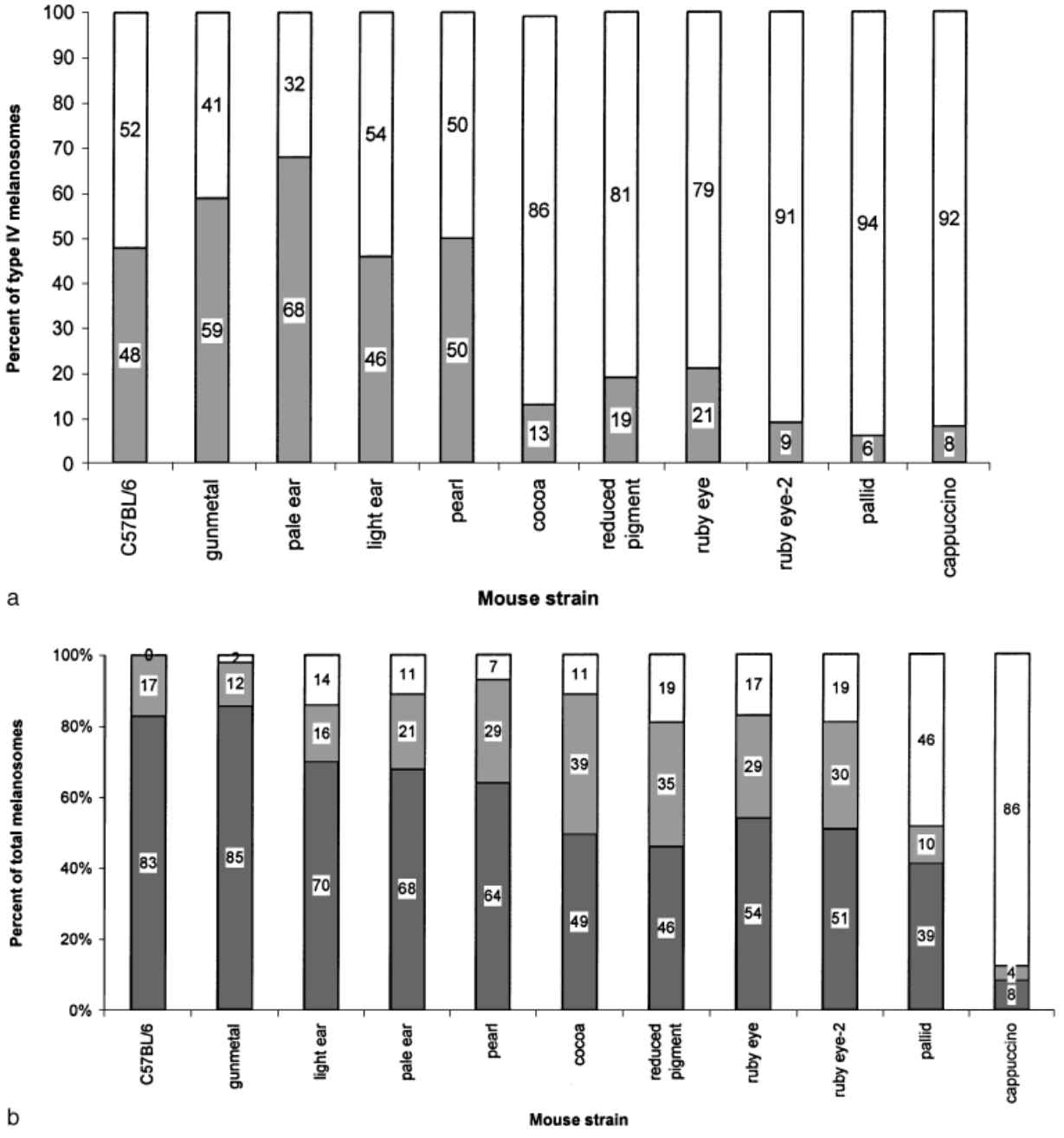

Figure 4. Melanosomes are shifted to immature forms in most HPS strains. (*a*) Type IV melanosomes classified by shape. *White bars*, percent of type IV melanosomes that are spherical. *Gray bars*, percent of type IV melanosomes that are elliptical. (*b*) Melanosomes classified by morphologic stage. *White bars*, percent of multivesicular bodies. *Light gray bars*, percent of melanosomes that are type II/III. *Dark gray bars*, percent of melanosomes that are type IV.

melanosomal transport or secretion (see *Discussion*). In contrast, the number of melanosomes per unit area in pale ear melanocytes was somewhat decreased compared with control cells, suggesting that no block in melanosome transport exists in this strain.

DISCUSSION

This study is a direct demonstration that HPS can be characterized by blocks in organelle development or transport. We observed that in many of the strains there was an increase in the percentage of immature forms relative to mature forms, suggesting that a rate-limiting step or block was introduced into the pathway of melanosome biogenesis.

The cappuccino and pallid strains exhibited an inhibition of melanosomal development at the earliest step, with cappuccino being the most severely affected. The accumulation of multivesicular structures in these strains is additional evidence that these structures are early precursors in melanosome biogenesis, possibly type I melanosomes (Raposo *et al*, 2001); this further confirms the close relationship between melanosomes and lysosomes (Orlow, 1995), which also have multivesicular bodies as precursors. As the predominant melanosome form in cappuccino has multivesicular morphology, and few striated and elongated shapes are observed, it appears that the Pmel17/gp100 protein may not be functioning normally in this strain. This may be due to a lack of cleavage of Pmel17/gp100, as it has been suggested that cleavage is required for striation formation (Raposo and Marks, 2002), or due to aberrant trafficking of the protein so that Pmel17/gp100 is not reaching the precursor melanosome.

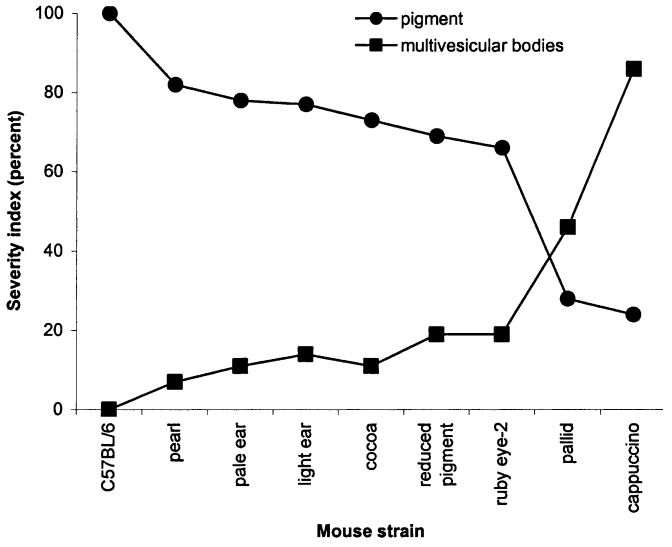

Figure 5. Degree of pigmentation varies inversely with degree of melanosomal maturity. Percent pigment dilution was calculated as detailed in *Materials and Methods*. Data for multivesicular bodies taken from **Fig 4(*b*)**.

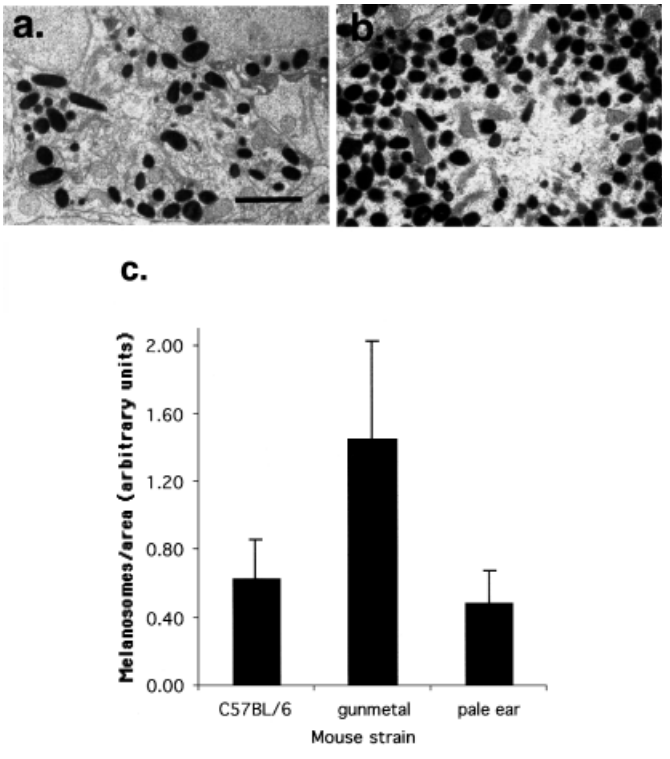

Figure 6. Melanosomes accumulate in gunmetal melanocytes. (*a*) C57BL/6, *scale bar* = 1.5 μm; (*b*) gunmetal; (*c*) number of melanosomes/unit area. Error bars represent SD.

The fact that pigment was observed in the immature forms in cappuccino indicates that at least a subset of the enzymes contributing to pigment production can be delivered to these compartments, as suggested previously (Kushimoto *et al*, 2001). This is consistent with studies demonstrating that when the tyrosinase gene is transfected into fibroblasts, tyrosinase protein is targeted to lysosomes, with pigment production (Bouchard *et al*, 1989; Winder *et al*, 1993). Thus the absence of a fully defined melanosomal compartment does not preclude delivery of pigment forming enzymes or pigment synthesis. It has been reported, however, that in normal type I melanosomes, proteolytic inactivation of pigment producing enzymes inhibits pigment from being produced in this compartment (Kushimoto *et al*, 2001), whereas in the cappuccino strain, the enzymes appear active, leading to pigment production. This suggests that the intralumenal pH in cappuccino precursor melanosomes may be abnormal, as an acidic environment may be necessary for proteolytic activity (Kushimoto *et al*, 2001; Raposo and Marks, 2002). It should be noted that the presence of pigment does not indicate that the protein trafficking of tyrosinase, Tyrp1/TRP-1, and dopachrome tautomerase/TRP-2 (enzymes involved in pigment synthesis) is normal. For example, in cells of patients with HPS2 (who have a defective AP3 subunit), it was shown that tyrosinase was mis-sorted but Tyrp1/TRP-1 was not (Huizing *et al*, 2001).

In one group of HPS strains, the two functions of the Pmel17/gp100 protein appear to have been dissociated, in that the intramelanosomal striations are clearly seen, but the melanosome appears blocked from progressing on to the elongated shape. Cocoa, ruby eye, ruby eye-2, and reduced pigmentation form a group in which there is an increase in the percentage of both multivesicular and type II/III forms, and a relative lack of elliptical type IV forms (**Fig 4**); most fully pigmented melanosomes in these strains are spherical. Additional factors that are necessary for elongation but not striation may not be targeted properly to the melanosome in these strains. For example, it is suggested that other proteins such as MART-1 may facilitate the functions of Pmel17/gp100 (De Maziere *et al*, 2002; Raposo and Marks, 2002). Alternatively, the Pmel17/gp100 protein undergoes a number of post-translational modifications such as glycosylation, cleavage, and interchain disulfide bond formation (Berson *et al*, 2001), and it is possible that Pmel17/gp100 processing is aberrant in these mutants, which may differentially affect the functions of the protein. The lack of elliptical forms in this group indicates that elliptical melanosomes derive from spherical precursors.

Several strains did not have a true block in melanosome development but rather the gene mutations in these strains (pearl, light ear, pale ear) seemed to introduce a rate-limiting step so that immature forms accumulated to a certain degree, but fully mature forms were also observed in abundance. The pearl strain was interesting in having membrane blebbing on fully pigmented ellipsoidal type IV forms; near these membranes were numerous vesicular structures (**Fig 2**, *pe*). The gene product is a subunit of the AP3 molecule, which is shown to function in vesicular trafficking at the *trans*-Golgi network and endosomal membranes. The effect of the mutation on melanosome maturation is modest, with an increase in type II/III forms, but many type IV forms are also seen (**Fig 4*b***), suggesting that a rate-limiting step is introduced between the transition from type II/III to type IV. It is possible that AP3 plays a part in delivering or sorting components to or from the type II/III or IV melanosome, and the pearl mutation impairs this trafficking, leading to a slowed transition from type II/III forms to type IV forms.

The gunmetal strain was unique among the strains examined here in accumulating increased numbers of relatively normal appearing intracellular melanosomes. This result is similar to that seen in cultured ashen melanocytes, which have a defective Rab27a (Wilson *et al*, 2000); melanosomes remain in the cell body and cannot be transported efficiently to the dendritic extensions (Bahadoran *et al*, 2001; Hume *et al*, 2001). Our results are also consistent with studies demonstrating that cytotoxic T cell granules in gunmetal are inefficiently targeted to the immunologic synapse (Stinchcombe *et al*, 2001). Together, these results suggest that melanosomes in gunmetal are accumulating due to either inefficient transport or secretion, and is unlikely due to increased synthesis of melanosomes. Recently, it was observed that cultured immortalized gunmetal melanocytes appeared to have fewer melanosomes than seen in control melanocytes (Zhang *et al*, 2002b). It is likely that this difference with our observations reported here is attributable to differences in melanocytes *in vivo vs* cultured cells, which have been selected by an immortalization process.

The mutation in gunmetal not only affects melanosomal transport, but also melanosomal size and maturation: the gunmetal melanosomes were smaller than those in control cells, and did not undergo a size increase from type II/III to type IV melanosomes. This is possibly due to the defective gene product in gunmetal affecting the prenylation of other rab proteins, in addition to Rab27a.

Two strains, pale ear and light ear, have melanosomes that are similar in appearance to one another and to wild-type melanosomes as well. This correlates with the observation that the body coat colors of both pale ear and light ear adult mice are dark and indistinguishable from one another (Swank *et al*, 1998), and that the pale ear gene product is not detectable in extracts from light ear cells, suggesting that the pale ear and light ear gene products function together in a complex (Suzuki *et al*, 2002). Similarly, ruby eye and ruby eye-2 are phenotypically indistinguishable, and the strains have very similar profiles of melanosome maturity. It does appear, however, that ruby eye can be distinguished from ruby eye-2 on the basis of average melanosome size.

Our findings of smaller melanosomes in the cocoa, pallid, and cappuccino strains are in agreement with previous studies that examined cultured melanocytes (Suzuki *et al*, 2001), skin tissue (Ito *et al*, 1982), and ocular tissue (Gwynn *et al*, 2000), respectively. Another study (Gardner *et al*, 1997) reported that pale ear cultured melanocytes contained melanosomes that were larger in size than seen in control melanocytes. This discrepancy with our observations can be explained by several factors. First, there may be differences due to examination of cultured cells *vs* melanocytes in tissue. Second, this study reports a statistical analysis of a large number of melanosomes, whereas the previous study selectively measured the largest melanosomes. It was also noted (Gardner *et al*, 1997; Suzuki *et al*, 2002) that pale ear and light ear had enlarged melanosomes in choroid melanocytes. This finding of larger melanosomes could be due to tissue-specific differences between melanocytes in the skin *vs* in the eye; melanocytes in the skin are secretory cells, whereas those in the eye are not known to secrete melanosomes. Alternatively the observational nature of the previous studies could account for the reported size differences; for example, the study of pallid (Ito *et al*, 1982) noted predominantly immature melanosomes in melanocytes, but occasional melanocytes with megamelanosomes.

The varying degrees to which melanosomal forms were shifted to immature, less pigmented forms (**Fig 4*b***) suggests a mechanism for the varying degrees of hypopigmentation seen in the HPS coat colors. As shown in **Fig 5**, an increase in the percentage of unpigmented multivesicular forms correlates with coat color dilution. Coat color is determined by the transfer of melanosomes into keratinocytes and subsequent incorporation into the hair shaft. Very little is known about the regulation of melanosome transfer, but we observed that immature melanosomal forms are transferred to keratinocytes (M.W. unpublished observations), indicating that secretion and uptake of melanosomes by keratinocytes is not limited to type IV forms. Thus, it is possible that hypopigmentation of the hair in most of these strains is caused by a dilution effect due to an increased percentage of relatively hypopigmented or unpigmented melanosomes being transferred; however, the hypopigmentation seen in gunmetal mice appears mainly due to retention of melanosomes in the melanocyte. Additionally, hypopigmentation may result from abnormal pigment synthesis, due to altered trafficking of selected enzymes or other components involved in pigment synthesis. It has been shown that transfection of HPS1 anti-sense cDNA into human melanoma cells caused mislocalization of tyrosinase and Tyrp1/TRP-1, and decreased melanin content (Sarangarajan *et al*, 2001). Also, when tyrosinase is routed to a compartment, such as the lysosome, which does not contain the full complement of proteins found in normal melanosomes, the pigment synthesized is pheomelanin, not eumelanin (Winder *et al*, 1993). It is not known if the biochemical composition of pigment in these HPS strains corresponds to that found in the control strains.

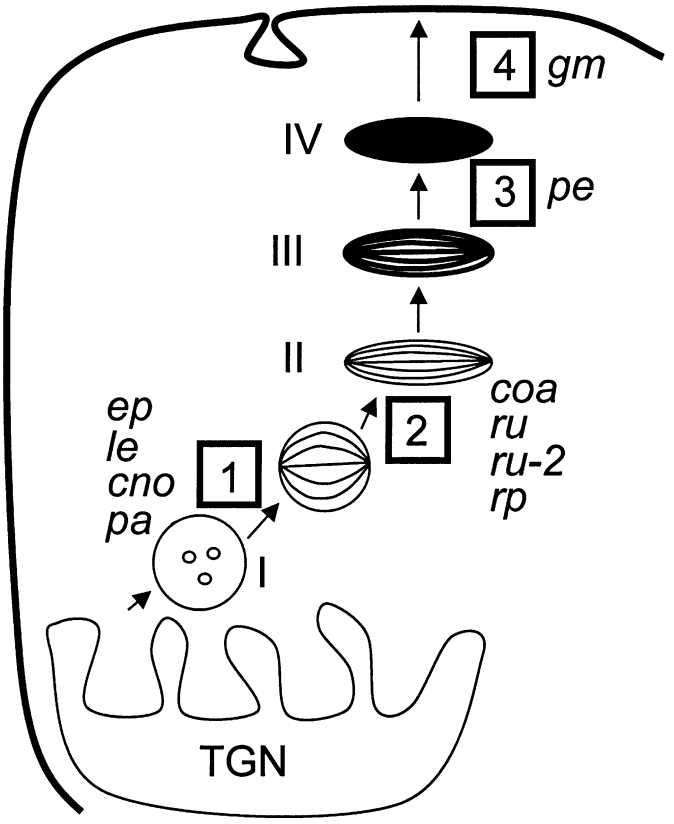

Figure 7. The morphologies of melanosomes in HPS strains reflect blocks in organelle biogenesis. The cappuccino (*cno*) mutation results in a proximal block (step 1) such that very few striated type II/III forms or fully pigmented forms are observed. The sizes of the organelles remain the size of precursor organelles, suggesting that pigment is being deposited in these early forms. The pallid (*pa*) mutation inhibits maturation at the same step as the cappuccino block. A more distal block (step 2) is predicted for the cocoa (*coa*), ruby eye (*ru*), ruby eye-2 (*ru-2*) and reduced pigmentation (*rp*) strains, as striated spherical forms are seen, but few ellipsoidal forms are noted. Accumulation of melanosomes in gunmetal (*gm*) melanocytes suggests that melanosomes are retained and inefficiently secreted (step 4). Introduction of a rate-limiting step, but not a true block in biogenesis, is predicted for pale ear and light ear (step 1), and pearl (step 3). Blebbing of melanosome limiting membrane in the pearl strain suggests that increased and/or slowed vesicular activity is occurring. TGN, *trans*-Golgi network.

In summary, we have examined melanosomes in HPS murine strains and classified the strains into categories that reflect the degree of melanosomal maturation. **Figure 7** depicts a proposed model that places the HPS protein products along the pathway of melanosomal biogenesis. Study of the murine melanosomes is useful in several ways. First, this quantitative *in vivo* assessment of the effects of HPS genes on a subcellular organelle shows clearly that these genes are involved in organelle maturation. Second, comparison of melanosome morphology from suspected HPS patients with melanosomes from murine strains could facilitate diagnosis of HPS. Currently, it is thought that many HPS patients are unrecognized and are diagnosed as having an unclassified bleeding disorder. To diagnose patients with HPS, bleeding time is measured, an ophthalmologic examination is done, and TEM analysis of platelets is performed. This last test is only available in one lab in the United States (Witkop *et al*, 1987), whereas TEM of a skin biopsy to examine melanosomes could be done using a few specialized university-based pathology laboratories with an interest in this area. Third, it is very likely that the HPS murine genes will be sequenced before the human genes, as the murine strains and corresponding chromosomal regions are already identified. By comparing patient melanosome morphology with murine HPS melanosome morphology, it may be possible

to classify human patients, to narrow down which chromosomal regions the defective genes are likely to reside, and to facilitate identification of the human HPS genes.

Many thanks to Drs Corey Largman and Regis Kelly for critical reading of the manuscript. We are grateful to Sandra Huling, Debra Crumrine, and Jerelyn Magnusson for excellent technical assistance. This work was supported by the Department of Veterans Administration (Research Career Development Award, M.L.W), also in part by National Institutes of Health (NIH HL55321, L.L.P.; HL51480, HL31698, EY12104, R.T.S.) and this research utilized core facilities supported in part by RPCI's NCI-funded Cancer Center Support Grant, CA16056.

REFERENCES

Bahadoran P, Aberdam E, Mantoux F, *et al*: Rab27a: a key to melanosome transport in human melanocytes. *J Cell Biol* 152:843–850, 2001

Banta LM, Robinson JS, Klionsky DJ, Emr SD: Organelle assembly in yeast, characterization of yeast mutants defective in vacuolar biogenesis and protein sorting. *J Cell Biol* 107:1369–1383, 1988

Berson JF, Harper DC, Tenza D, Raposo G, Marks MS: Pmel17 initiates premelanosome morphogenesis within multivesicular bodies. *Mol Biol Cell* 12:3451–3464, 2001

Bouchard B, Fuller BB, Vijayasaradhi S, Houghton AN: Induction of pigmentation in mouse fibroblasts by expression of human tyrosinase cDNA. *J Exp Med* 169:2029–2042, 1989

Chavrier P, Goud B: The role of ARF and Rab GTPases in membrane transport. *Curr Opin Cell Biol* 11:466–475, 1999

De Maziere AM, Muehlethaler K, Van Donselaar E, *et al*: The melanocytic protein melan-A/MART-1 has a subcellular localization distinct from typical melanosomal proteins. *Traffic* 3:678–693, 2002

Dell'Angelica EC, Shotelersuk V, Aguilar RC, Gahl WA, Bonifacino JS: Altered trafficking of lysosomal proteins in Hermansky–Pudlak syndrome due to mutations in the beta 3A subunit of the AP-3 adaptor. *Mol Cell* 3:11–21, 1999

Dell'Angelica EC, Mullins C, Caplan S, Bonifacino JS: Lysosome-related organelles. *FASEB J* 14:1265–1278, 2000

Detter JC, Zhang Q, Mules EH, *et al*: Rab geranylgeranyl transferase alpha mutation in the gunmetal mouse reduces Rab prenylation and platelet synthesis. *Proc Natl Acad Sci USA* 97:4144–4149, 2000

Faundez V, Horng JT, Kelly RB: A function for the AP3 coat complex in synaptic vesicle formation from endosomes. *Cell* 93:423–432, 1998

Feng L, Seymour AB, Jiang S, *et al*: The beta3A subunit gene (Ap3b1) of the AP-3 adaptor complex is altered in the mouse hypopigmentation mutant pearl, a model for Hermansky–Pudlak syndrome and night blindness. *Hum Mol Genet* 8:323–330, 1999

Gardner JM, Wildenberg SC, Keiper NM, *et al*: The mouse pale ear (ep) mutation is the homologue of human Hermansky–Pudlak syndrome. *Proc Natl Acad Sci USA* 94:9238–9243, 1997

Gibb S, Hakansson EM, Lundin LG, Shire JG: Reduced pigmentation (rp), a new coat colour gene with effects on kidney lysosomal glycosidases in the mouse. *Genet Res* 37:95–103, 1981

Gwynn B, Ciciotte SL, Hunter SJ, *et al*: Defects in the cappuccino (cno) gene on mouse chromosome 5 and human 4p cause Hermansky–Pudlak syndrome by an AP-3-independent mechanism. *Blood* 96:4227–4235, 2000

Huang L, Kuo YM, Gitschier J: The pallid gene encodes a novel, syntaxin 13-interacting protein involved in platelet storage pool deficiency. *Nat Genet* 23: 329–332, 1999

Huizing M, Anikster Y, Gahl WA: Hermansky–Pudlak syndrome and related disorders of organelle formation. *Traffic* 1:823–835, 2000

Huizing M, Sarangarajan R, Strovel E, Zhao Y, Gahl WA, Boissy RE: AP-3 mediates tyrosinase but not TRP-1 trafficking in human melanocytes. *Mol Biol Cell* 12:2075–2085, 2001

Hume AN, Collinson LM, Rapak A, Gomes AQ, Hopkins CR, Seabra MC: Rab27a regulates the peripheral distribution of melanosomes in melanocytes. *J Cell Biol* 152:795–808, 2001

Ito M, Hashimoto K, Organisciak DT: Ultrastructural, histochemical, and biochemical studies of the melanin metabolism in eye and skin of pallid mice. *J Invest Dermatol* 78:414–424, 1982

Kantheti P, Qiao X, Diaz ME, *et al*: Mutation in AP-3 delta in the mocha mouse links endosomal transport to storage deficiency in platelets, melanosomes, and synaptic vesicles. *Neuron* 21:111–122, 1998

Kushimoto T, Basrur V, Valencia J, *et al*: A model for melanosome biogenesis based on the purification and analysis of early melanosomes. *Proc Natl Acad Sci USA* 98:10698–10703, 2001

Nordlund JJ, Boissy RE, Hearing VJ, King RA, Ortonne JP: *The Pigmentary System. Physiology and Pathophysiology.* New York: Oxford University Press, 1998

Novak EK, Wieland F, Jahreis GP, Swank RT: Altered secretion of kidney lysosomal enzymes in the mouse pigment mutants ruby-eye, ruby-eye-2-J, and maroon. *Biochem Genet* 18:549–561, 1980

Novak EK, Hui SW, Swank RT: Platelet storage pool deficiency in mouse pigment mutations associated with seven distinct genetic loci. *Blood* 63:536–544, 1984

Novak EK, Sweet HO, Prochazka M, *et al*: Cocoa: a new mouse model for platelet storage pool deficiency. *Br J Haematol* 69:371–378, 1988

Novick P, Zerial M: The diversity of Rab proteins in vesicle transport. *Curr Opin Cell Biol* 9:496–504, 1997

Orlow SJ: Melanosomes are specialized members of the lysosomal lineage of organelles. *J Invest Dermatol* 105:3–7, 1995

Raposo G, Marks MS: The dark side of lysosome-related organelles: specialization of the endocytic pathway for melanosome biogenesis. *Traffic* 3:237–248, 2002

Raposo G, Tenza D, Murphy DM, Berson JF, Marks MS: Distinct protein sorting and localization to premelanosomes, melanosomes, and lysosomes in pigmented melanocytic cells. *J Cell Biol* 152:809–824, 2001

Raymond CK, Howald-Stevenson I, Vater CA, Stevens TH: Morphological classification of the yeast vacuolar protein sorting mutants: evidence for a prevacuolar compartment in class E vps mutants. *Mol Biol Cell* 3:1389–1402, 1992

Sarangarajan R, Budev A, Zhao Y, Gahl WA, Boissy RE: Abnormal translocation of tyrosinase and tyrosinase-related protein 1 in cutaneous melanocytes of Hermansky–Pudlak syndrome and in melanoma cells transfected with anti-sense HPS1 cDNA. *J Invest Dermatol* 117:641–646, 2001

Seiji M, Fitzpatrick T, Simpson R, Birbeck M: Chemical composition and terminology of specialized organelles (melanosomes and melanin granules) in mammalian melanocytes. *Nature* 197:1082–1084, 1963

Stinchcombe JC, Barral DC, Mules EH, *et al*: Rab27a is required for regulated secretion in cytotoxic T lymphocytes. *J Cell Biol* 152:825–834, 2001

Suzuki T, Li W, Zhang Q, *et al*: The gene mutated in cocoa mice, carrying a defect of organelle biogenesis, is a homologue of the human Hermansky–Pudlak syndrome-3 gene. *Genomics* 78:30–37, 2001

Suzuki T, Li W, Zhang Q, *et al*: Hermansky–Pudlak syndrome is caused by mutations in HPS4, the human homolog of the mouse light-ear gene. *Nat Genet* 30: 321–324, 2002

Swank RT, Novak EK, McGarry MP, Rusiniak ME, Feng L: Mouse models of Hermansky Pudlak syndrome: a review. *Pigment Cell Res* 11:60–80, 1998

Wada Y, Ohsumi Y, Anraku Y: Genes for directing vacuolar morphogenesis in *Saccharomyces cerevisiae* . I. Isolation and characterization of two classes of vam mutants. *J Biol Chem* 267:18665–18670, 1992

Wilson SM, Yip R, Swing DA, *et al*: A mutation in Rab27a causes the vesicle transport defects observed in ashen mice. *Proc Natl Acad Sci USA* 97:7933–7938, 2000

Winder AJ, Wittbjer A, Rosengren E, Rorsman H: Fibroblasts expressing mouse c locus tyrosinase produce an authentic enzyme and synthesize phaeomelanin. *J Cell Sci* 104:467–475, 1993

Witkop CJ, Krumwiede M, Sedano H, White JG: Reliability of absent platelet dense bodies as a diagnostic criterion for Hermansky–Pudlak syndrome. *Am J Hematol* 26:305–311, 1987

Zhang Q, Li W, Novak EK, *et al*: The gene for the muted (mu) mouse, a model for Hermansky–Pudlak syndrome, defines a novel protein which regulates vesicle trafficking. *Hum Mol Genet* 11:697–706, 2002a

Zhang Q, Zhen L, Li W, *et al*: Cell-specific abnormal prenylation of Rab proteins in platelets and melanocytes of the gunmetal mouse. *Br J Haematol* 117:414–423, 2002b